Uncoupling of growth plate maturation and bone formation in mice lacking both Schnurri-2 and Schnurri-3

Dallas C. Jones[a,b,1], Michelle N. Schweitzer[a], Marc Wein[a], Kirsten Sigrist[a], Tsuyoshi Takagi[c], Shunsuke Ishii[c], and Laurie H. Glimcher[a,b,d,1]

[a]Department of Immunology and Infectious Disease, Harvard School of Public Health, Boston, MA 02115; [b]Department of Medicine, Harvard Medical School, Boston, MA 02115; [c]Laboratory of Molecular Genetics, RIKEN Tsukuba Institute, Tsukuba, Ibaraki 305-0074, Japan; and [d]Ragon Institute of Massachusetts Institute of Technology, Massachusetts General Hospital, and Harvard, Boston, MA 02129

Contributed by Laurie H. Glimcher, March 22, 2010 (sent for review March 5, 2010)

Formation and remodeling of the skeleton relies on precise temporal and spatial regulation of genes expressed in cartilage and bone cells. Debilitating diseases of the skeletal system occur when mutations arise that disrupt these intricate genetic regulatory programs. Here, we report that mice bearing parallel null mutations in the adapter proteins Schnurri2 (Shn2) and Schnurri3 (Shn3) exhibit defects in patterning of the axial skeleton during embryogenesis. Postnatally, these compound mutant mice develop a unique osteochondrodysplasia. The deletion of Shn2 and Shn3 impairs growth plate maturation during endochondral ossification but simultaneously results in massively elevated trabecular bone formation. Hence, growth plate maturation and bone formation can be uncoupled under certain circumstances. These unexpected findings demonstrate that both unique and redundant functions reside in the Schnurri protein family that are required for proper skeletal patterning and remodeling.

chondrodysplasia | osteoblast | skeletogenesis

Formation of the skeleton is a complex biological process that requires coordination of numerous molecular and cellular networks at a myriad of unique anatomical sites (1, 2). Based on the anatomical location, the generation of these various skeletal elements will arise through one of two distinct ossification processes. The flat bones in the skull and medial clavicle are formed through intramembranous ossification, which occurs when mesenchymal stem cells differentiate directly into osteoblasts (3, 4). The remaining bones of the axial and appendicular skeleton are produced through endochondral ossification. Skeletal elements formed through the endochondral process require the formation of an intermediate cartilaginous scaffold from which the future ossified bone will be derived (5, 6).

Proper temporal and spatial formation of the cartilaginous template generated during endochondral ossification results from a highly ordered chondrogenic program that occurs in the growth plates of the developing bones (7). In response to specific microenvironmental cues, chondrocytes residing in an epiphyseal pool of resting cells begin to proliferate and orient themselves into columns along a longitudinal axis where they synthesize a matrix rich in type II collagen. As the chondrocytes continue to develop and move further down this axis, they exit from the cell cycle, become hypertrophic, and generate an extracellular matrix comprised largely of type X collagen (8). Terminally differentiating chondrocytes also secrete factors that promote neovascularization of the cartilaginous scaffold. The formation of blood vessels allows for the influx of cells required to complete the ossification process. Osteoblasts are among the cells that colonize the recently vascularized cartilage. Infiltration of these cells from the perichondrium is essential for the replacement of the cartilaginous template as osteoblasts generate the extracellular constituents required to form trabecular bone (9). Therefore, endochondral bone formation is thought to require a synchronization of chondrogenesis, osteogenesis, and vascularization.

The Schnurri family of large zinc-finger proteins consists of three mammalian homologs (Shn1, Shn2, and Shn3) that are present in numerous tissue and cell types, including those within the skeleton (10–17). Recent analysis of mice deficient in individual *Shn* genes has uncovered a novel role for this protein family in regulating skeletal remodeling. Mice lacking Shn2 display a modest low-turnover osteopenia that is the result of reduced osteoclast and osteoblast function (16). In stark contrast to these findings, we have recently described an extreme osteosclerotic phenotype present in $Shn3^{-/-}$ mice due to increased osteoblast activity and elevated bone formation rates (11). The divergent skeletal phenotypes of the $Shn2^{-/-}$ and $Shn3^{-/-}$ mice led us to further explore the relationship between these proteins in the skeletal system by generating compound mutant mice lacking both Shn2 and Shn3. Analysis of these compound mutant mice revealed an unexpected cooperative function of Shn2 and Shn3 within various skeletal cell types. Mice lacking Shn2 and Shn3 develop a chondrodysplastic phenotype resulting from altered growth plate biology that is not observed in mice lacking only one of these genes. Unexpectedly, the chondrodysplastic Shn2/3-compound mutant animals simultaneously exhibit an accelerated onset and progression of the osteoslcerotic phenotype observed in $Shn3^{-/-}$ mice. Hence, Shn2/3-compound mutant mice provide a novel model of endochondral ossification where formation of trabecular bone is uncoupled from growth plate biology. These findings reveal novel functions of the Schnurri protein family in skeletal biology.

Results and Discussion

Deletion of Shn2 and Shn3 Results in Growth Defects and Skeletal Pathology. We hypothesized that compensatory functions may exist between Shn2 and Shn3 in tissues where expression of these two genes overlaps. To address this, we used previously characterized $Shn2^{-/-}$ mice and $Shn3^{-/-}$ mice to generate compound mutant mice deficient in both Shn2 and Shn3 (Shn2/3-DKO) (10–13, 16, 17). Shn2/3-DKO mice are indistinguishable from control littermates at birth but thereafter display a severe growth retardation that results in a dwarfed phenotype, and do not survive beyond 3 weeks of age (Fig. 1*A* and *B*). Examination of skeletal preparations revealed that the dwarfism in Shn2/3-DKO mice arises from shortening of both axial and appendicular skeletons (Fig. 1*C*). Our subsequent analysis of the axial skeleton uncovered patterning defects in the Shn2/3-DKO vertebrae and sternum. As shown in Fig. 1 *D* and *E*, spinous

Author contributions: D.C.J., M.N.S., and L.H.G. designed research; D.C.J., M.N.S., and K.S. performed research; D.C.J., M.N.S., M.W., T.T., S.I., and L.H.G. analyzed data; and D.C.J. and L.H.G. wrote the paper.

Conflict of interest statement: L.H.G. is a member of the Board of Directors of and holds equity in the Bristol Myers Squibb Corporation.

[1]To whom correspondence may be addressed. E-mail: lglimche@hsph.harvard.edu or djones@hsph.harvard.edu.

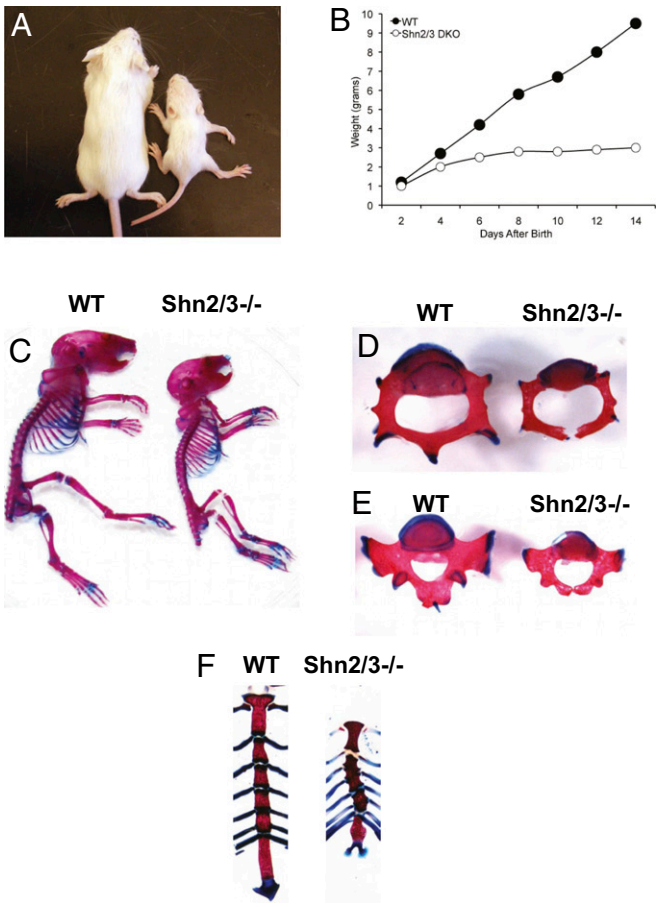

Fig. 1. Skeletal patterning defects in mice lacking Shn2 and Shn3. (*A*) Dwarfed phenotype of Shn2/3-DKO mouse (*Right*) when compared with WT control (*Left*). (*B*) Growth curve of WT (filled circle) and Shn2/3-DKO mice (open circle) from P0 to P14 (*C*) Alizarin red– and alcian blue–stained skeletal preparations of 2-week-old WT and Shn2/3-DKO mice. Comparison of (*D*) lumbar and (*E*) thoracic vertebrae isolated from Shn2/3-DKO mice and WT mice. (*F*) Irregular sternalcostal junctions are also observed in Shn2/3-DKO mice.

processes were absent from lumbar and thoracic vertebrae of Shn2/3-DKO mice. The incomplete formation of these vertebrae also resulted in a nonossified gap being present along the vertebral dorsal midline (Fig. 1 *D* and *E*). The absence of Shn2 and Shn3 also resulted in impaired sternum development, as abnormal sternocostal junctions were commonly observed in Shn2/3-DKO mice (Fig. 1*F*). These results further expand the previously established role for Shn2 and Shn3 in skeletal remodeling by describing an unknown function for Shn2 and Shn3 in skeletal patterning.

Growth Plate Abnormalities in Mice Deficient for Shn2 and Shn3. Analysis of proximal and distal bones isolated from the limbs of Shn2/3-DKO mice revealed a remarkable shortening when compared with WT bones (Fig. 2*A*). Given the central role of chondrocyte proliferation and differentiation indictating the growth of long bones, we analyzed femurs isolated from WT neonatal mice for expression of Shn2 and Shn3 by in situ hybridization. As shown in Fig. 2 *B* and *C*, expression of Shn2 and Shn3 in the growth plate was detected in both proliferating and hypertrophic chondrocyte populations. Based on the overlapping expression of Shn2 and Shn3 in the different chondrocyte populations, we next asked whether there was any discernible pathology at the growth plate of the Shn2/3-DKO mice. Histological examination of the distal femoral growth plates revealed the hypertrophic zone of the Shn2/3-DKO mice to be disorganized and smaller when compared with the hypertrophic zone of WT mice (Fig. 2 *D*–*G*). A reduction in the size of the Shn2/3-DKO hypertrophic zone was further confirmed by in situ hybridization for type X collagen (ColX), a marker specific for hypertrophic chondrocytes (Fig. 2 *H* and *I*).

In other murine models of chondrodysplasia, reductions in chondrocyte proliferation often are observed in concert with defects in chondrocyte maturation (18). To determine whether chondrocyte proliferation was altered in Shn2/3-DKO mice, we assessed BrdU incorporation into the growth plates of Shn2/3-DKO mice and littermate controls. As shown in Fig. 2 *J*–*M*, the epiphyseal growth plate of femurs isolated from Shn2/3-DKO mice 6 h after BrdU injection showed a marked reduction in the number of BrdU positive cells within the proliferative zone when compared with the growth plates of control littermates.

Reductions in chondrocyte proliferation coupled with alterations in differentiation that are observed in the Shn2/3-DKO mice are consistent with other dwarfism phenotypes that arise in mice through chondrodysplasia. Defects in chondrocyte biology also result in delayed formation of the secondary ossification center that is often observed in chondrodysplastic phenotypes (18–20). Indeed, the formation of the secondary ossification center in the epiphysis of the Shn2/3-DKO femurs was also delayed (Fig. 2 *D* and *E*). To address whether the appearance of the primary ossification center was also delayed, we isolated limbs from E16.5 Shn2/3-DKO and control littermates. Histological analysis of the E16.5 limbs revealed an established primary ossification center in both Shn2/3-DKO and control littermates with no discernible difference observed in limb size and morphology between these two groups (Fig. 2 *N* and *O*).

We sought to confirm that Shn2 and Shn3 function in a cell-intrinsic manner to control chondrocyte maturation. For this, we used lentiviral transduction to ectopically express either Shn2 or Shn3 in the chondrogenic cell line ATDC5. In addition to expressing Shn2 or Shn3, these lentiviruses also carry a puromycin resistance cassette that allows for the selection of successfully infected cells following treatment with puromycin. The lentiviral-infected ATDC5 cells were then cultured under conditions previously described that promote their differentiation through the hypertrophic phase, which can be determined by analyzing Col X expression (21). As shown in Fig. 2*P*, ectopic expression of either Shn2 or Shn3 in ATDC5 cells resulted in augmented levels of Col X expression when measured kinetically over a 21-day period. Collectively, these results suggest that Shn2 and Shn3 can function intrinsically to regulate chondrocyte proliferation and maturation and further expands the significant role of this protein family in skeletal biology.

Persistence of High Bone Mass Phenotype in Shn2/3-DKO Mice. Skeletal elements formed through endochondral ossification are derived from cartilaginous templates that are replaced by osteoblast derived bone matrix. Decreases in bone mass are therefore frequently observed in mice with genetic mutations that impede the formation of the cartilaginous template through a disruption in chondrocyte biology (22–24). Accordingly, we anticipated that the osteosclerotic phenotype that we previously reported to be present in the Shn3$^{-/-}$ strain would not be preserved in the chondrodysplastic Shn2/3-DKO mice (11). However, examination of long bones harvested from 2-week-old WT, Shn2$^{-/-}$, Shn3$^{-/-}$, and Shn2/3-DKO mice revealed, unexpectedly, that a high–bone mass phenotype was still present in the Shn2/3-DKO mice (Fig. 3*A*). In addition, the onset of this skeletal phenotype was accelerated in the Shn2/3-DKO mice. Long bones isolated from 2-week-old Shn2/3-DKO mice already exhibited markedly increased trabecular bone volume in comparison with age-matched Shn3$^{-/-}$ mice, which displayed only a modest increase in trabecular bone volume at that age (Fig. 3*A*). Further analysis of the femurs isolated from Shn2/3-DKO mice by μCT revealed that the extensive trabecular network extended well into the diaphyseal region where it appeared to be emanating from the endosteal surface (Fig. 3 *B* and *C*). In situ hybridization revealed that the trabecular

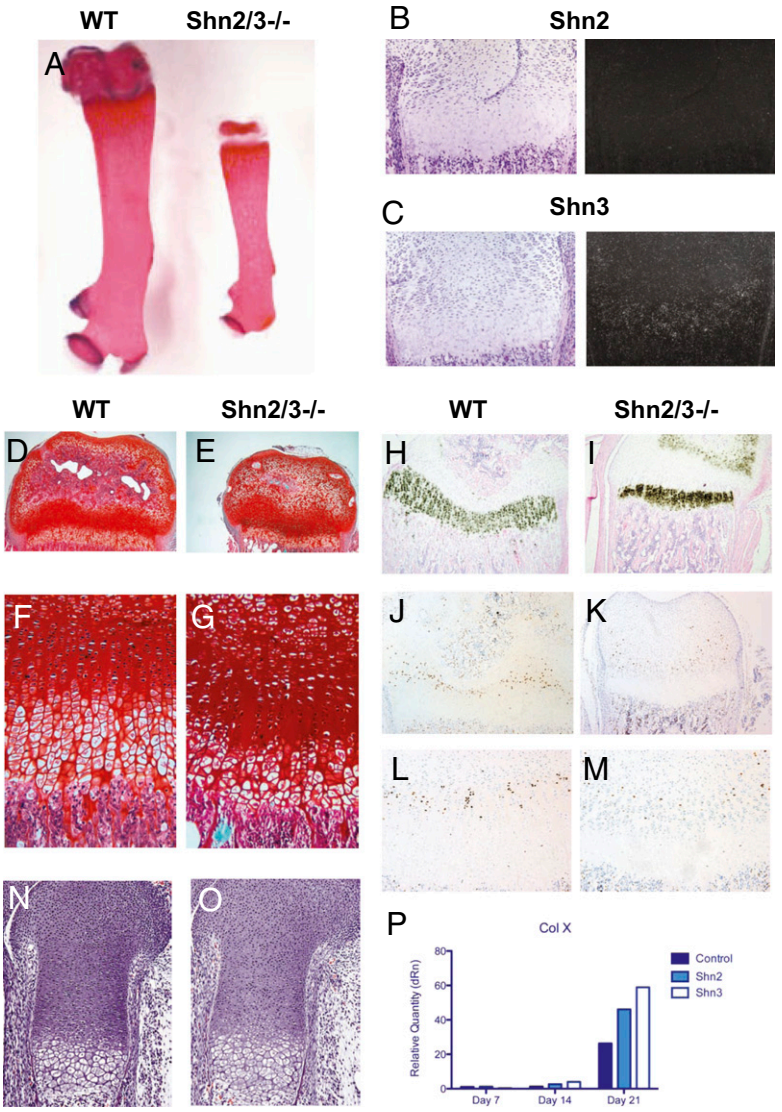

Fig. 2. Histological analysis of the growth plates from Shn2/3-DKO mice. (*A*) Alizarin red and alcian blue staining of femurs isolated from 2-week-old WT and Shn2/3-DKO mice. In situ hybridization depicting the expression of (*B*) Shn2 and (*C*) Shn3 in the growth plate of the distal femur. Safranin O–stained histological sections from the distal femur of (*D* and *F*) WT and (*E* and *G*) Shn2/3-DKO mice. Detection of Col X expression by in situ hybridization in the distal femur of (*H*) WT and *(I)* Shn2/3-DKO mice. Detection of BrdU-labeled chondrocytes in the distal femoral growth plate of (*J* and *L*) WT and *(K* and *M)* Shn2/3-DKO mice. *(L* and *M)* Higher magnifications of growth plate. H&E staining of limbs isolated from (*N*) WT and (*O*) Shn2/3-DKO mice at E16.5. (*P*) Expression of Col X is measured in ATDC5 cells transduced with control, Shn2, or Shn3 expressing lentivirus via qPCR every 7 days over a 3-week period.

bones in this distal region of the Shn2/3-DKO femurs were lined with cells expressing canonical osteoblast markers such as osteocalcin and type I collagen, suggesting that the increased bone mass arose from augmented osteoblast activity (Fig. 3 *D* and *E*) and similar to what we had previously observed in single Shn3$^{-/-}$ mice (11).

The extensive trabecular network present in the long bones of the Shn2/3-DKO mice could also arise through a failure of osteoclasts to resorb the primary spongiosa. Decreased osteoclast differentiation and/or function may result in trabecular bones consisting of calcified cartilage. To address this, we analyzed histological tissue sections of WT and Shn2/3-DKO femurs that were stained with toluidine blue to detect the presence of calcified cartilage. As shown in Fig. 3*F*, trabecular bone in the femurs of WT mice is located in close proximity to the growth plate where it was extensively stained for toluidine blue. In contrast, the numerous trabeculae that are located in the diaphyseal regions of the Shn2/3-DKO femurs are toluidine blue negative, suggesting that the cartilaginous template has been effectively resorbed in the Shn2/3-DKO femurs and replaced with osteoblast-derived lamellar bone (Fig. 3 *G* and *H*). To further address whether osteoclastogenesis was impaired in the Shn2/3-DKO mice, we analyzed femurs from age-matched WT and Shn2/3-DKO mice for the presence of tartrate-resistant acid phosphatase–positive (TRAP-positive) osteoclasts. In comparison with age-matched WT controls, Shn2/3-DKO mice showed similar numbers of TRAP-positive cells providing additional evidence that the increased trabecular bone mass in the Shn2/3-DKO mice does not arise from a perturbation of osteoclast activity (Fig. 3 *I* and *J*). Collectively, these results provide a unique demonstration of endochondral bone formation where the formation of trabecular bones can occur in long bones that also exhibit impaired growth plate maturation.

Onset of Chondrodysplasia and Elevated Bone Mass Exhibit Differing Sensitivities to Schnurri Gene Dosage. We observed during the generation and characterization of the Shn2/3-compound mutant mice that the growth defects identified in the Shn2/3-DKO mice were not present in mice containing only a single copy of Shn2

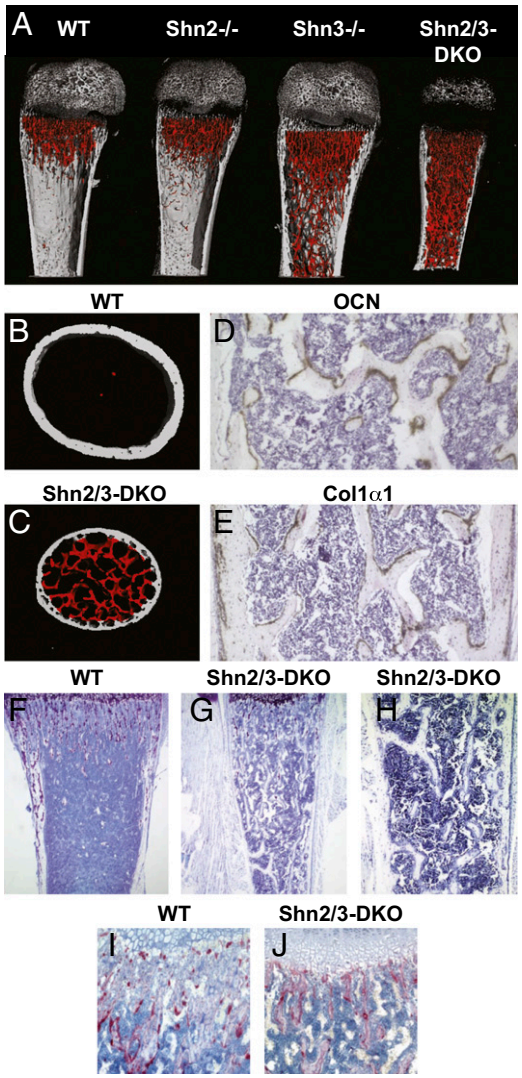

Fig. 3. Shn2/3-DKO mice exhibit elevated trabecular bone mass. (*A*) False colored three-dimensional μ-QCT image demonstrating the various degrees of trabecular bone in the distal femurs isolated from WT, $Shn2^{-/-}$, $Shn3^{-/-}$ and Shn2/3-DKO mice. Additional false-colored μCT image of diaphysial region of (*B*) WT and (*C*) Shn2/3-DKO femurs showing trabecular bone in red. In situ hybridization detecting the presence of (*D*) osteocalcin (OCN) and (*E*) type 1 collagen (Col1α1) positive cells lining the trabeculae in the diaphysis of Shn2/3-DKO femurs. Toluidine blue stained tissue sections from (*F*) WT and (*G*) Shn2/3-DKO femurs. (H) High magnification of the midshaft region of Shn2/3-DKO femur. Detection of TRAP-positive osteoclasts at the growth plate of (I) WT and (J) Shn2/3-DKO mice.

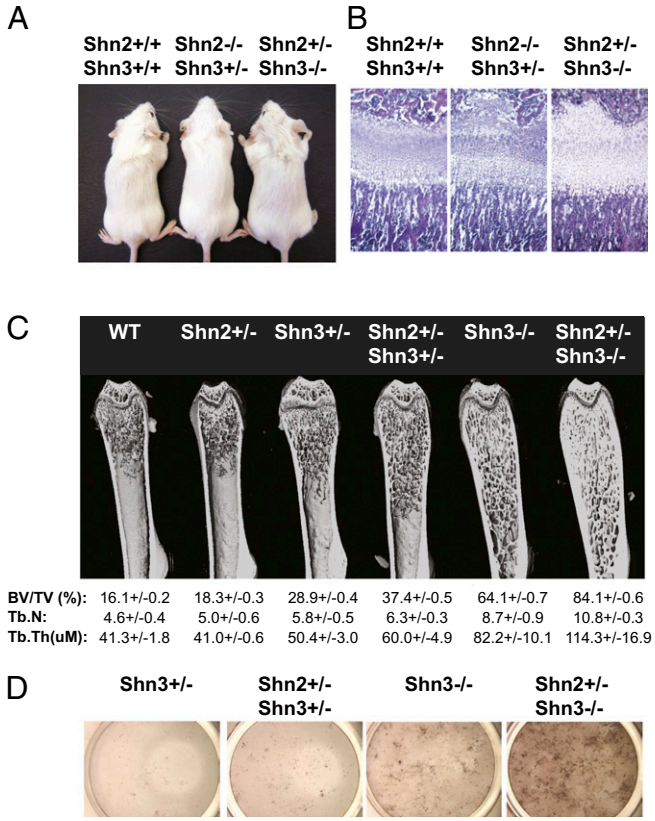

Fig. 4. Effects of Schnurri gene dosage on growth plate and trabecular bone formation. (*A*) Photograph of 5-week-old WT, $Shn2^{-/-}Shn3^{+/-}$ and $Shn2^{+/-}Shn3^{-/-}$ mice. (*B*) H&E staining of distal femoral growth plate of WT, $Shn2^{-/-}Shn3^{+/-}$, and $Shn2^{+/-}Shn3^{-/-}$ mice. (*C*) 3D μ-QCT images of the distal femurs isolated from the various Shn2/3-compound mutant mice. Below, analysis of the μ-QCT images for bone volume per tissue volume (BV/TV), trabecular number (Tb.N.) and trabecular thickness (Tb.Th.). (*D*) von Kossa staining of bone marrow stromal cultures generated from $Shn3^{+/-}$, $Shn2^{+/-}Shn3^{+/-}$, $Shn3^{-/-}$, and $Shn2^{+/-}Shn3^{-/-}$ mice.

($Shn2^{+/-}Shn3^{-/-}$) or a single copy of Shn3 ($Shn2^{-/-}Shn3^{+/-}$) (Fig. 4*A*). Accordingly, the growth plate architecture of the $Shn2^{+/-}Shn3^{-/-}$ and $Shn2^{-/-}Shn3^{+/-}$ mice was comparable to that of WT mice and did not display any of the pathological characteristics seen in the Shn2/3-DKO mice (Fig. 4*B*). These findings indicate that complete ablation of both Shn2 and Shn3 is necessary to perturb growth plate maturation. In contrast, deletion of a single Shn3 allele ($Shn3^{+/-}$) was sufficient to cause an increase in bone mass. Moreover, deletion of a single copy of Shn2 in parallel with a single copy of Shn3 ($Shn2^{+/-}Shn3^{+/-}$) resulted in a further augmentation of this bone mass phenotype (Fig. 4*C*). Analysis of the femurs isolated from $Shn2^{+/-}Shn3^{-/-}$ mice revealed a BV/TV that was 5-fold that of the WT controls (Fig. 4*C*). These data demonstrate that bone formation is highly sensitive to Schnurri gene dosage in vivo.

To determine whether differences in Schnurri gene dosage could also alter osteoblast function in vitro, we generated bone marrow stromal cultures from 5-week-old $Shn3^{+/-}$, $Shn2^{+/-}Shn3^{+/-}$, $Shn3^{-/-}$, and $Shn2^{+/-}Shn3^{-/-}$ mice. Kinetic analysis of matrix production by von Kossa staining over a 14-day period revealed that stromal cultures generated from $Shn2^{+/-}Shn3^{-/-}$ mice produced the highest levels of mineralized matrix (Fig. 4*D*). Further reflecting the in vivo findings, we also observed that $Shn2^{+/-}Shn3^{+/-}$ stromal cultures produced elevated levels of mineralized matrix when compared with the $Shn3^{+/-}$ cultures. These data reveal gradients of skeletal remodeling that are exquisitely sensitive to Shn2 and Shn3 gene expression. A 50% reduction in expression of either gene can have an impact on both osteoblast function in vitro and bone formation in vivo.

In conclusion, we describe a previously uncharacterized osteochondrodysplasia present in mice bearing parallel null mutations in Shn2 and Shn3. The growth plate defects that are observed in the Shn2/3-DKO mice share similarities with other murine models of chondrodysplasia; however, the Shn2/3-DKO mice are unique in that an increased trabecular bone mass is observed in the same skeletal elements where chondrocyte proliferation and maturation is disrupted. Furthermore, the presence of this phenotype in the Shn2/3-DKO mice but its absence in either $Shn2^{-/-}Shn3^{+/+}$ or $Shn2^{+/+}Shn3^{-/-}$ mice suggests that a compensatory role for Shn2 and Shn3 exists within the skeletal system. In addition to Shn2 and

Shn3, previous reports have demonstrated that Shn1 is also expressed at specific sites within the skeleton (25). It is possible that a compensatory increase in Shn1 expression in the Shn2/3-compound mutant mice may contribute to the phenotype observed in the skeleton of these compound mutant mice. Analysis of Shn1-deficient mice as well as Shn1/Shn2, Shn1/Shn3, and Shn1/Shn2/Shn3-compound mutant mice will be required to determine whether Shn1 has a role in regulating skeletal biology either independently of or in parallel with the other Schnurri family members. Further research directed at elucidating both the unique and overlapping roles of the Schnurri protein family within cells of the skeletal system will provide a fuller understanding of endochondral bone formation.

Materials and Methods

Animals. Compound Shn2/3-mutant mice were generated using the previously described strains of Shn3$^{-/-}$ mice and Shn2$^{-/-}$ mice (11, 17). Animals were maintained in accordance with the National Institutes of Health *Guide for the Care and Use of Laboratory Animals* and were handled according to protocols approved by the institution's subcommittee on animal care.

Skeletal Preparation. Mice were skinned, eviscerated, and dehydrated in 95% ETOH overnight. The samples were then transferred into acetone for an additional 48-h incubation. Skeletal preparations were stained for 4 days using alcian blue and alizarin red as described previously (26). Following staining, the samples were washed for 30 min three times in 95% ETOH. The soft tissue was then cleared in 1% KOH.

μCT Imaging and Analysis. Proximal femurs were isolated from WT and Shn2/3-compound mutant mice and fixed in 70% ethanol. A region 0.28 mm proximal to the distal growth plate was scanned using a Scanco Medical μCT 35 system (Scanco) with a spatial resolution of 7μm. From these scans, a region of 2.1 mm in length of the distal metaphysis was selected for analysis. Images were reconstructed into 3D volumes with the region of interest being segmented using a fixed threshold. Unbiased, 3D microstructural properties of trabecular bone, including bone volume fraction, trabecular thickness, trabecular number, trabecular separation were then calculated for the trabecular region of the metaphysis of the distal femur using methods based on distance transformation of the binarized images.

Histology and in Situ Hybridization. Generation and preparation of skeletal tissue for histological analysis and in situ hybridization were performed as described previously (27). In situ probes for collagen X, collagen I, and osteocalcin were kindly provided by Beate Lanske. Digoxigenine-labeled RNA probes were then generated by T7 or T3 RNA polymerase according to the manufacturer's protocol. Transcript specific probes for Schnurri-2 and Schnurri-3 were generated by subcloning cDNA fragments into pBluescript. ^{35}S-UTP–labeled riboprobes complementary for Shn2 and Shn3 were then generated and used for performing in situ hybridization following previously established protocols (28).

ACKNOWLEDGMENTS. The authors thank Dorothy Zhang for expert histology preparation, Drs. Yukiko Maeda and Despina Sitara for technical assistance with in situ hybridization, and Nicholas Brady for generation of μCT images and analysis. This work was supported by National Institutes of Health Grants HD055601 (to L.H.G.) and K99AR055668 (to D.C.J.) and by a grant from Merck Pharmaceuticals.

1. Erlebacher A, Filvaroff EH, Gitelman SE, Derynck R (1995) Toward a molecular understanding of skeletal development. *Cell* 80:371–378.
2. Karsenty G, Wagner EF (2002) Reaching a genetic and molecular understanding of skeletal development. *Dev Cell* 2:389–406.
3. Cohen MM, Jr (2000) Merging the old skeletal biology with the new. I. Intramembranous ossification, endochondral ossification, ectopic bone, secondary cartilage, and pathologic considerations. *J Craniofac Genet Dev Biol* 20:84–93.
4. Dunlop LL, Hall BK (1995) Relationships between cellular condensation, preosteoblast formation and epithelial-mesenchymal interactions in initiation of osteogenesis. *Int J Dev Biol* 39:357–371.
5. Mackie EJ, Ahmed YA, Tatarczuch L, Chen KS, Mirams M (2008) Endochondral ossification: How cartilage is converted into bone in the developing skeleton. *Int J Biochem Cell Biol* 40:46–62.
6. Ortega N, Behonick DJ, Werb Z (2004) Matrix remodeling during endochondral ossification. *Trends Cell Biol* 14:86–93.
7. Kronenberg HM (2003) Developmental regulation of the growth plate. *Nature* 423: 332–336.
8. Noonan KJ, Hunziker EB, Nessler J, Buckwalter JA (1998) Changes in cell, matrix compartment, and fibrillar collagen volumes between growth-plate zones. *J Orthop Res* 16:500–508.
9. Caplan AI, Pechak DG (1987) The cellular and molecular embryology of bone formation. *Bone and Mineral Research*, ed Peck WA (Elsevier, New York), 5:117–184.
10. Jin W, et al. (2006) Schnurri-2 controls BMP-dependent adipogenesis via interaction with Smad proteins. *Dev Cell* 10:461–471.
11. Jones DC, et al. (2006) Regulation of adult bone mass by the zinc finger adapter protein Schnurri-3. *Science* 312:1223–1227.
12. Kimura MY, et al. (2005) Regulation of T helper type 2 cell differentiation by murine Schnurri-2. *J Exp Med* 201:397–408.
13. Kimura MY, et al. (2007) Schnurri-2 controls memory Th1 and Th2 cell numbers in vivo. *J Immunol* 178:4926–4936.
14. Oukka M, et al. (2002) A mammalian homolog of Drosophila schnurri, KRC, regulates TNF receptor-driven responses and interacts with TRAF2. *Mol Cell* 9:121–131.
15. Oukka M, Wein MN, Glimcher LH (2004) Schnurri-3 (KRC) interacts with c-Jun to regulate the IL-2 gene in T cells. *J Exp Med* 199:15–24.
16. Saita Y, et al. (2007) Lack of Schnurri-2 expression associates with reduced bone remodeling and osteopenia. *J Biol Chem* 282:12907–12915.
17. Takagi T, Harada J, Ishii S (2001) Murine Schnurri-2 is required for positive selection of thymocytes. *Nat Immunol* 2:1048–1053.
18. Naski MC, Colvin JS, Coffin JD, Ornitz DM (1998) Repression of hedgehog signaling and BMP4 expression in growth plate cartilage by fibroblast growth factor receptor 3. *Development* 125:4977–4988.
19. Chen M, et al. (2008) Inhibition of beta-catenin signaling causes defects in postnatal cartilage development. *J Cell Sci* 121:1455–1465.
20. Lee HH, Behringer RR (2007) Conditional expression of Wnt4 during chondrogenesis leads to dwarfism in mice. *PLoS One* 2(5):e450.
21. Shukunami C, et al. (1997) Cellular hypertrophy and calcification of embryonal carcinoma-derived chondrogenic cell line ATDC5 in vitro. *J Bone Miner Res* 12: 1174–1188.
22. Bonaventure J, et al. (1992) Type II collagen defect in two sibs with the Goldblatt syndrome, a chondrodysplasia with dentinogenesis imperfecta, and joint laxity. *Am J Med Genet* 44:738–753.
23. Forlino A, et al. (2005) A diastrophic dysplasia sulfate transporter (SLC26A2) mutant mouse: Morphological and biochemical characterization of the resulting chondrodysplasia phenotype. *Hum Mol Genet* 14:859–871.
24. Maeda Y, et al. (2007) Indian Hedgehog produced by postnatal chondrocytes is essential for maintaining a growth plate and trabecular bone. *Proc Natl Acad Sci USA* 104:6382–6387.
25. Tanaka K, Matsumoto Y, Nakatani F, Iwamoto Y, Yamada Y (2000) A zinc finger transcription factor, alphaA-crystallin binding protein 1, is a negative regulator of the chondrocyte-specific enhancer of the alpha1(II) collagen gene. *Mol Cell Biol* 20: 4428–4435.
26. McLeod MJ (1980) Differential staining of cartilage and bone in whole mouse fetuses by alcian blue and alizarin red S. *Teratology* 22:299–301.
27. Shim JH, et al. (2009) TAK1 is an essential regulator of BMP signalling in cartilage. *EMBO J* 28:2028–2041.
28. Sitara D, et al. (2004) Homozygous ablation of fibroblast growth factor-23 results in hyperphosphatemia and impaired skeletogenesis, and reverses hypophosphatemia in Phex-deficient mice. *Matrix Biol* 23:421–432.